Study Title

Indirect Photolysis of Gaseous Perfluorooctanesulfonyl Fluoride (POSF)
by Fourier Transform Infrared (FTIR) Spectroscopy

Data Requirement:

Based on Literature Review

Author

Grant M. Plummer, Ph.D.

Study Completion Date

June 12, 2001

Performing Laboratory

3M Environmental Laboratory
Building 2-3E-09, 935 Bush Avenue
St. Paul, MN 55106

Project Identification

3M Laboratory Report No. E01-0739

Total Number of Pages

38

This page has been reserved for specific country requirements.

Statement of Non-Compliance

Study Title: Indirect Photolysis of Gaseous Perfluorooctanesulfonyl Fluoride (POSF) by Fourier Transform Infrared (FTIR) Spectroscopy

Study Identification Number: E01-0739

This study does not comply with the requirements of the US EPA Good Laboratory Practices (GLP) Standards at 40 CFR Part 792 (TSCA).

Author Date 06/12/01

Sponsor Date 06/12/01

Table of Contents

List of Tables

List of Figures

Study Personnel and Contributors

Author

Grant M. Plummer, Ph.D.
Rho Squared
PO Box 61536
Durham, NC 27715
(919) 682-4761

Sponsor

William K. Reagen, Ph.D.
3M Environmental Laboratory
Bldg. 2-3E-09, 35 Bush Avenue
St. Paul, MN 55133-3331
(651) 778-6565

3M Environmental Laboratory and Professional Services Contributing Personnel

Timothy Gutzkow
Pace Analytical Services, Inc., 1700 Elm St., Minneapolis, MN 55144

Location of Archives

The 3M Environmental Laboratory will retain the original data documents and digital copies of the original data related to this work for at least 10 years following the effective date of any related final ruling. Information may be obtained through written inquiry addressed as follows:

3M Environmental Laboratory
Building 2-3E-09
935 Bush Avenue
St. Paul, MN 55106

Summary

The primary goal of this study was to determine the first order reaction rate of gaseous perfluorooctanesulfonyl fluoride (hereafter, POSF) with the gaseous hydroxyl radical (hereafter, OH) at one atmosphere total pressure and 33° C.

Several publications[1, 2, 3, 4] describing related measurements formed the experimental and theoretical basis of this study. Members of the 3M Environmental Laboratory and other contributing personnel developed the equipment and analytical techniques required to perform the study.

Our results are based on the relative gaseous concentrations of POSF and the reference compound monochloromethane (hereafter, CH_3Cl) in the presence of the OH radical. We performed the concentration measurements using continuous, in-situ Fourier transform infrared (FTIR) spectroscopic techniques.

The study data generally indicate *that no reactions between POSF and the OH radical occur in the gas phase.* Within first order kinetic theory, and in conjunction with the results of independent studies of CH_3Cl and OH, the results of one run (*only*) performed in this study establish an estimated *minimum* half-life of POSF related to its reactions with the OH radical. That estimate is, under typical tropospheric conditions, 3.7 years.

Introduction

The environmental mobility and fate of a chemical are controlled by a number of natural processes, including volatilization, bioaccumulation, biodegradation, oxidation, reduction, hydrolysis, and photolysis. This work concerns the rate of indirect photolysis of the gaseous form of the compound POSF through its reactions with the gaseous hydroxyl radical OH. Figure 1 illustrates the structure of POSF.

"Indirect photolysis" is the process by which gas phase radicals are formed in the atmosphere in presence of ultraviolet (UV) radiation and subsequently react with other chemical species. The gas phase reaction with the hydroxyl radical OH is one of several mechanisms by which organic compounds, both natural and synthetic, decompose in the environment. The radical OH and other radicals are present in the troposphere, but only at concentrations below the detection limits of most continuous analytical methods.

This work describes an experimental investigation of the indirect photolysis of POSF. The gas test matrix employed in this study consisted of percent levels of O_2, H_2O, O_3, and He, as well as the compounds CH_3Cl and POSF at levels below 100 ppm. The matrix was subject to UV and visible radiation in the $\lambda \geq 200$ nm wavelength range. Reference 1 describes in detail the reactions by which the OH radical is produced under such conditions.

Figure 1. Structure of POSF

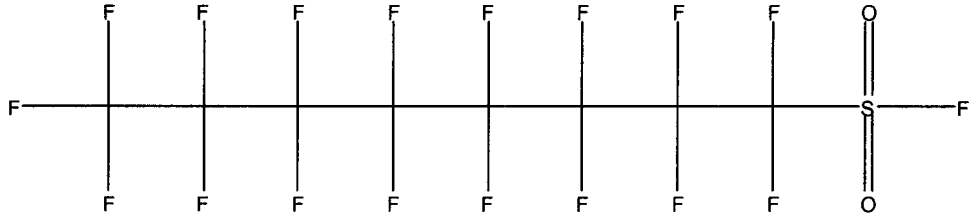

Kinetics Model

As mentioned above, OH radicals exist in the troposphere at concentrations below the detection limits of most continuous analytical methods; this is often true even in the most carefully prepared laboratory gas matrices. However, the concentration of the OH radical in a well-characterized test matrix can be indirectly determined from behavior of a reference compound R (in this study, CH_3Cl) for which the first-order OH reaction rate constant k_{R1} is already well known. As described below, this approach allows an estimate of the first-order rate constant k_{A1} for the analyte A (in this study, POSF).

In the experiments described here, we introduced ozone (O_3) and water (H_2O) into a series of the test matrices containing POSF and CH_3Cl; when subject to ultraviolet (UV) radiation, these first two molecules react to form the OH radical.[1] The OH radical can then react with and photolytically degrade the analyte and the reference compounds. We noted minor losses in the concentrations of ozone $[O_3]$, the analyte $[A]$, and the reference compound $[R]$ in the absence of UV radiation; we assume below that these losses were caused by adsorption to or reactions between these compounds and the reaction chamber walls.

A model describing the reactions, the first order (or pseudo-first order) rate laws, and the rate constants considered in this work are described below.

Reaction	Rate	
$A + OH \Rightarrow (Products)_A$	$k_{A1}[A][OH]$	Eqs. (1), (2)
$A \Rightarrow (Wall\ Losses)_A$	$k_{A2}[A]$	Eqs. (3), (4)
$R + OH \Rightarrow (Products)_R$	$k_{R1}[R][OH]$	Eqs. (5), (6)
$R \Rightarrow (Wall\ Losses)_R$	$k_{R2}[R]$	Eqs. (7), (8)
$O_3 + H_2O + h\nu \Rightarrow 2OH + O_2$	$k_{O1}[O_3]$	Eqs. (9), (10)
$O_3 \Rightarrow (Wall\ Losses)_O$	$k_{O2}[O_3]$	Eqs. (11), (12)

We note that this model assumes that the reference and analyte compounds do not undergo direct photolysis, that is, that their concentrations are unaffected by the

presence of the UV radiation except through the described mechanisms involving the hydroxyl radical. Equation 10 also assumes that water is present in excess.

In each experimental run, the UV intensity and the concentration $[OH]$ were zero for the period $0 \le t \le t'$ and non-zero for times $t > t'$. Equations describing the measured quantities $[O_3]$, $[R]$, and $[A]$ as a function of time for each of these conditions are derived below.

According to Equations 9 through 12, the differential equations governing the O_3 concentrations are

$$d[O_3]_t = -[O_3]_t \, k_{O2} \, dt \qquad (0 \le t \le t')$$

Eq. (13a)

$$d[O_3]_t = -[O_3]_t (k_{O1} + k_{O2}) \, dt \qquad (t > t')$$

Eq. (13b)

where the subscript t denotes the concentrations at all times. The solutions to these equations are

$$[O_3]_t = [O_3]_0 \exp\{-k_{O2} t\} \qquad (0 \le t \le t')$$

Eq. (14a)

$$[O_3]_t = [O_3]_{t'} \exp\{-(k_{Oi} + k_{O2})(t - t')\} \qquad (t > t')$$

Eq. (14b)

where the subscripts 0 and t' and denote the concentrations at times $t = 0$ and $t = t'$.

We assume below that, under each experimental condition and only in the presence of UV radiation, the OH concentration is proportional to the O_3 concentration. Although the radical OH is extremely reactive, this is a reasonable assumption for our description of the reactions of Equations 1 and 5. The hydroxyl radical concentration is then given by the following expressions:

$$[OH]_t = 0 \qquad (0 \le t \le t')$$

Eq. (15a)

$$[OH]_t = \alpha [O_3]_{t'} \exp\{-(k_{O1} + k_{O2})(t - t')\} \qquad (t > t')$$

Eq. (15b)

where α is constant and we have employed the initial condition $[OH]_{t'} = \alpha [O_3]_{t'}$ at time $t = t'$.

According to the reaction model and assumptions described above, the differential equations governing the analyte concentrations are

$$d[A]_t = -[A]_t(k_{A2})\,dt \qquad (0 \le t \le t')$$

Eq. (16a)

$$d[A]_t = -[A]_t\left(k_{A2} + k_{A1}[OH]_{t'}\right)dt \qquad (t > t')$$

$$= -[A]_t\left(k_{A2} + k_{A1}\alpha[O_3]_{t'}\exp\{-(k_{O1}+k_{O2})(t-t')\}\right)dt$$

Eq. (16b)

Direct integration of Equation 16a gives the solution for $0 \le t \le t'$ (UV = 0):

$$\ln\left[\frac{[A]_t}{[A]_0}\right] = -k_{A2}t \qquad (0 \le t \le t')$$

Eq. (17)

under initial condition $[A]_t = [A]_0$ at time $t = 0$.

Subject to the condition that $k_{O1} + k_{O2} \neq 0$, direct integration of Equation 16b gives the general solution of Equation 16b for $t > t'$ (UV ≠0):

$$\ln[A]_t = C - k_{A2}t + \frac{k_{A1}\,\alpha\,[O_3]_{t'}}{k_{O1}+k_{O2}}\exp\{-(k_{O1}+k_{O2})(t-t')\} \qquad (t > t')$$

Eq. (18)

and evaluation the constant of integration C at time $t = t'$ yields the specific solution

$$\ln\left[\frac{[A]_t}{[A]_{t'}}\right] = -k_{A2}(t-t') - \frac{k_{A1}\,\alpha\,[O_3]_{t'}}{k_{O1}+k_{O2}}\left[1-\exp\{-(k_{O1}+k_{O2})(t-t')\}\right] \qquad (t > t')$$

Eq. (19)

Using the same assumptions and analogous initial conditions, the reference compound concentrations are given by

$$\ln\left[\frac{[R]_t}{[R]_0}\right] = -k_{R2}t \qquad (0 \le t \le t')$$

Eq. (20)

and

$$\ln\left[\frac{[R]_t}{[R]_{t'}}\right] = -k_{R2}(t-t') - \frac{k_{R1}\,\alpha\,[O_3]_{t'}}{k_{O1}+k_{O2}}\left[1-\exp\{-(k_{O1}+k_{O2})(t-t')\}\right] \qquad (t > t')$$

Eq. (21)

For $t > t'$, Equations 19 and 21 yield the following expression for the ratio k_{A1}/k_{R1}:

$$\frac{k_{A1}}{k_{R1}} = \frac{\ln([A]_t/[A]_{t'}) + k_{A2}(t-t')}{\ln([R]_t/[R]_{t'}) + k_{R2}(t-t')} \qquad \text{Eq. (22)}$$

in which the four quantities related to [A] and [R] are experimentally accessible. When $k_{A2} = k_{R2} = 0$, an estimate of the ratio k_{A1}/k_{R1} can be directly calculated from the observed concentrations[3].

In our experiments, the condition $k_{A2} = k_{R2} = 0$ did not hold. Therefore, Equation 22 and our experimental data do not provide an accurate estimate of the ratio k_{A1}/k_{R1}.

Accordingly, we used Equations 3, 4, 11, and 13 in a series of direct least-squares analyses. In these analyses, we adjusted the parameters representing the rate constants of Equations 2, 4, 6, 8, 10, and 12 according to the differences between the observed and calculated values of the concentrations [A], [R], and $[O_3]$. Equations 14, 17, 19, 20, and 21 generated the calculated concentrations, and values of the parameters were varied to the minimize the sum square error (SSE)

$$\mathrm{SSE} = \sum_{m,j} \left(A_m^j - \hat{A}_m^j\right) \qquad \text{Eq. (23)}$$

where the index m indicates the three observed compounds POSF, CH_3Cl,and O_3 (m = 1 to 3, respectively) and the index j enumerates the normalized concentrations A_m^j and their least squares estimates $\hat{A}_m^j$. The normalized concentrations are the observed concentrations divided by each compound's initial (t = 0) concentration.

The analysis yield the four least-squares rate constant estimates $\tilde{k}_{O1}$, $\tilde{k}_{O2}$, $\tilde{k}_{A2}$, and $\tilde{k}_{R2}$, as well as estimates of the two quantities (see Equations 19 and 21)

$$\tilde{K}_{A1} = \frac{k_{RA}\,\alpha\,[O_3]_{t'}}{k_{O1} + k_{O2}} \qquad \text{Eq. (24)}$$

and

$$\tilde{K}_{R1} = \frac{k_{R1}\,\alpha\,[O_3]_{t'}}{k_{O1} + k_{O2}} \quad . \qquad \text{Eq. (25)}$$

An experimental estimate of the quantity

$$\hat{k}_{R1} = 3.6 \times 10^{-14}\ \mathrm{cm^3\ sec^{-1}} \qquad \text{Eq. (26)}$$

is available in the literature[2], so our experimental estimate of the first-order reaction rate constant $\hat{k}_{A1}$ is (see Equation 23)

$$\tilde{k}_{A1} \approx \frac{\tilde{K}_{A1}}{\tilde{K}_{R1}} \hat{k}_{R1} \quad . \qquad \text{Eq. (27)}$$

Using the estimated value of Equation 27, the analyte concentration in the absence of wall effects (i.e. when $k_{A2} = 0$) and in the presence of a constant hydroxyl radical concentration $[OH]$ (for instance, in the Earth's lower atmosphere) obeys

$$[A]_t = -[A]_0 \exp\left\{-\hat{k}_{A1}[OH]t\right\}. \qquad \text{Eq. (28)}$$

Under these conditions, our experimental estimate of the analyte half-life is given by

$$\tilde{T}_{1/2} = \frac{\ln(2)}{\tilde{k}_{A1}[OH]}. \qquad \text{Eq. (29)}$$

Materials and Methods

Method Summary

We prepared and analyzed the samples included in this study between August 8 and August 24, 2000; our techniques were based on those described in References 1, 2, 3, and 4. We performed all the measurements described here in a combination reaction chamber and infrared absorption cell developed and patented by 3M Corporation[5]. For this study, the cell was equipped with a capacitance barometer (Kurt J. Lesker Company, Model KJL-902056) and a polished, semi-conductor-grade quartz window (Glass Tech Supplies, Inc.) through which UV radiation from a broad-band discharge lamp (Ariel Inc., Model #6269) was introduced to the reagent gases. The temperature of the chamber was maintained at 33°C. Except for the infrared mirror faces, we manually cleaned the interior surfaces of the cell with acetone before each sample preparation. We added reagents to the chamber after first evacuating it to pressures below 100 mTorr, and determined the resulting mixture concentrations from the original gas standard concentrations and the barometric measurements. We generated O_3 by illuminating a 40% - 60% gaseous mixture of O_2 and helium (He) with a short-wavelength UV source in a separate reaction chamber (Thermo Environmental, Inc. NO_x Analyzer, Model 42C) and transferred the resulting gas, which contained approximately 1% O_3, to the reaction chamber/IR absorption cell.

Chemical Characterizations

Table 1 lists the properties the test and reference materials used in this study.

Table 1. Characterizations of the Test and Reference Substances

Test or Reference Substance	POSF	O_2/He	CH_3Cl/He	He	H_2O
Source	3M Environmental Laboratory	Oxygen Services Company	Oxygen Services Company	Oxygen Services Company	3M Environmental Laboratory
Expiration Date	N/A	7/27/2001	7/27/2001	N/A	N/A
Storage Conditions	Silcosteel canister, ambient T, 30 psig	steel cylinder, ambient temperature, ~2100 psig	steel cylinder, ambient temperature, ~2100 psig	steel cylinder, ambient temperature, ~2100 psig	Pyrex sample tube, ambient T and P
Cylinder or Lot Number	12517LB	00-564-L	SG9123566	OSC38878	N/A

Sample Preparation and Analysis

We prepared all the samples used in this study using barometric measurements; all reagents were introduced into the experimental apparatus as gases. Table 2 describes the control conditions and concentrations.

Table 2. Run Designations and Experimental Conditions

				Reagent Pressures (Torr)				
Run Designation	Control/ Sample Condition	Data Set	UV (Watts)	O_3[A]	H_2O	O_2/He	POSF	CH_3Cl/He
C1A	UV = 0	T11A	0	16	6	655	9	100
C1B	High UV	T11B	600	16	6	655	9	100
C2A	[A]= 0; UV = 0	T12A	0	17	6	664	0	100
C2B	[A] = 0	T12B	300	17	6	664	0	100
C3A	[R]= 0; UV = 0	T13A	0	19	6	755	9	0
C3B	[R] = 0	T13B	300	19	6	755	9	0
C4A	High [R]; UV = 0	T14A	0	9	6	355	9	400
C4B	High [R]	T14B	300	9	6	355	9	400
C5A	High [A]; UV = 0	T15A	0	16	6	628	36	100
C5B	High [A]	T15B	300	16	6	628	36	100
S1A	Sample Run #1; UV = 0	T8A	0	16	6	655	9	100
S1B	Sample Run #1	T8B	300	16	6	655	9	100
S2A	Sample Run #2; UV = 0	T17A	0	16	6	655	9	100
S2B	Sample Run #2	T17B	300	16	6	655	9	100

[A]Estimated from the input O_2 concentration and manufacturers' stated ozonator efficiency for air at flow rates of one liter per minute (2.5%).

Results and Discussion

Statistical Methods and Calculations

Using functions provided in Microsoft® Excel® software, we have used the kinetics model described above to form estimates of the rate constants $\tilde{k}_{O1}$, $\tilde{k}_{O2}$, $\tilde{k}_{A2}$, and $\tilde{k}_{R2}$, as well as estimates of the two quantities $\tilde{K}_{A1}$ and $\tilde{K}_{R1}$ (see Equations 24 through 27). The estimates presented below for each sample and control condition described in Table 3 are those leading to a minimum in the related sum square error in the normalized concentrations described in Equation 23. In our performance of these least-squares analyses, we constrained the parameter $\tilde{K}_{A1}$ to non-negative values, and found no other parametric constraints necessary.

The reaction chamber/IR absorption cell provides an infrared absorption pathlength of 10 meters for monitoring the reagent concentrations. We used a MIDAC™ Model I2001 FTIR spectrometer and associated software (AutoQuant™ V3.11) to acquire infrared absorbance spectra of the gaseous mixtures. The nominal spectral resolution of the system is 0.5 cm^{-1}, and it employs a mercury-cadmium-telluride (MCT) detector operated at 77K. We confirmed the system absorption pathlength through comparisons of experimental spectra to those of the National Institute for Standards and Technology (NIST) spectral database spectrum of ethylene.

We determined relative concentrations of POSF, CH_3Cl, and O_3 using a classical least squares (CLS) spectral analysis technique within AutoQuant™. The analytical regions employed (in cm^{-1}) were 1101.6 – 1320.7, 2824.5 – 3012.7, and 2052.5 – 2141.7, respectively; all these analyses employed linear baseline corrections. Appendix A portrays the CLS results; Appendix B illustrates the reference spectra and analytical regions. The concentration values of Appendix A have been independently and arbitrarily scaled to allow a clear graphical representation of the concentration trends, and do not represent the actual concentrations.

The actual volumetric part-per-million concentrations of the three compounds on which we have based our results varied greatly over the required control and sample conditions. To avoid bias in the least squares analyses, which are sensitive to the absolute concentration values, we normalized each concentration by dividing it by the first concentration value used in the analyses. These normalized concentrations are represented in the figures of Appendix C, which also illustrate our analytical results.

Data Summary and Discussion

Table 3 lists the results of the least squares analyses of the normalized concentration data for POSF, CH_3Cl, and O_3 under four control conditions and two sample conditions.

Table 3. Least Squares Estimates of the Rate Constants and Ratios

Run/Control Designation	Control Condition	$\tilde{k}_{A2}$ (A)	$\tilde{K}_{A1}$ (B)	$\tilde{k}_{R2}$ (A)	$\tilde{K}_{R1}$ (B)	$\tilde{k}_{O2}$ (A)	$\tilde{k}_{O1}$ (A)
C1	High UV	1.78×10^{-3}	0	2.31×10^{-2}	3.52×10^{-3}	2.00×10^{-3}	9.58×10^{-2}
C2	[A] = 0	N/A	N/A	5.46×10^{-3}	1.38×10^{-2}	1.51×10^{-3}	5.75×10^{-2}
C3	[R]= 0	1.06×10^{-3}	0	N/A	N/A	1.11×10^{-3}	5.28×10^{-2}
C4	High [R]	9.15×10^{-4}	2.17×10^{-3}	3.12×10^{-3}	1.29×10^{-2}	1.05×10^{-3}	6.09×10^{-2}
C5	High [A]	1.07×10^{-3}	0	8.30×10^{-3}	2.72×10^{-3}	6.09×10^{-4}	4.09×10^{-2}
S1	None	1.52×10^{-3}	0	5.73×10^{-3}	1.28×10^{-2}	3.28×10^{-3}	4.90×10^{-2}
S2	None	7.84×10^{-4}	0	8.86×10^{-3}	7.14×10^{-3}	1.45×10^{-3}	5.39×10^{-2}

[A] In units min^{-1}.

[B] In units $cm^3\ min^{-1}$.

Table 3 demonstrates the variability in the parameters $\tilde{k}_{A2}$, $\tilde{k}_{R2}$, and $\tilde{k}_{O2}$ over the course of our experiments. These parameters describe losses of the compounds that are not related to the presence of UV radiation, and may have been caused by interactions with the sample chamber walls. As described above, the magnitude and variability of these parameters prevent accurate application of Equation 22. The least squares results of Table 3 are based on a single mathematical constraint, namely, that $\tilde{K}_{A1}$ was required to remain non-negative.

In all but one case (that of control condition C4) the value of $\tilde{K}_{A1}$ leading to the least squares solutions was "bound" to the value zero. This means that, in these cases, the value $\tilde{K}_{A1} = 0$ leads to the minimum model error (SSE) under the (single) constraint $\tilde{K}_{A1} \geq 0$, and that the majority of the experimental data (three control runs and two sample runs) show no degradation of POSF. *Therefore, the main finding of this work is that POSF does not undergo indirect photolysis in the presence of the hydroxyl radical.*

The available data do not explain why the results of control condition C4, under which the concentration of the reference compound (CH_3Cl) was elevated, should lead to a detectable decrease in the POSF concentration. A plausible explanation is that the reference compound, through either direct or indirect photolysis, produced other radicals (including, possibly, the Cl radical) that do react with and lead to the degradation of POSF. Such an effect might only be apparent under conditions such as those of run C4, with relatively high CH_3Cl concentration.

If we nonetheless assume that the observed (Run C4) degradation was caused by the hydroxyl radical alone, then an estimate of the half-life of POSF related to its gas phase

reactions with the hydroxyl radical alone is available. Table 4 presents the details of the related calculation.

Table 4. Estimated Minimum Atmospheric Half-Life of POSF Due to Gas Phase Reaction with the Hydroxyl Radical Based Only on Run C4 Data.

Quantity	Dimensions	Value	Reference
Run C4 rate ratio $\tilde{K}_{R1}$	$cm^3\ min^{-1}$	1.29E-02	Eq. (25)
Run C4 rate ratio $\tilde{K}_{A1}$	$cm^3\ min^{-1}$	2.17E-03	Eq. (24)
Known Rate Constant $\hat{k}_{R1}$	$cm^3\ sec^{-1}$	3.60E-14	(2)
Calculated Rate Constant $\tilde{k}_{A1}$	$cm^3\ sec^{-1}$	6.06E-15	Eq. (27)
Known [OH] in lower atmosphere	cm^{-3}	9.70E+05	(3)
Rate $\{\tilde{k}_{R1}$ [OH] $\}$	sec^{-1}	5.87E-09	Eq. (29)
$\tilde{T}_{1/2}$ for POSF	seconds	1.18E+08	Eq. (29)
$\tilde{T}_{1/2}$ for POSF	years	3.74E+00	Eq. (29)

Because *only* the Run C4 data indicate a non-zero value of $\tilde{K}_{A1}$, we consider the $\tilde{T}_{1/2}$ value presented in Table 4 (3.7 years) as the minimum value POSF half-life supported by the study data.

Conclusions

We have performed a study of the indirect photolysis of perfluorooctanesulfonyl fluoride (POSF) in the gas phase. The primary goal of this study was to determine a first order reaction rate constant describing the gas phase reactions between POSF and the hydroxyl radical at 33° C and one atmosphere total pressure.

Our results are based on the relative gaseous concentrations of POSF and the reference compound monochloromethane (CH_3Cl) in the presence of OH and ultraviolet (UV) radiation. We performed the concentration measurements using continuous, in-situ Fourier transform infrared (FTIR) spectroscopic techniques.

Six of the seven control and sample runs we performed indicated no degradation of POSF in the presence of the OH radical. Therefore, our main finding is that reactions between POSF and the OH radical do not occur in the Earth's atmosphere. However, in one control run only, we observed a slight decrease in the POSF concentration. The relative rates of degradation of POSF and CH_3Cl observed in this single run, in conjunction with as a previously published[1] rate for the CH_3Cl – OH reaction, are consistent with a POSF half-life of 3.7 years in the presence of typical tropospheric concentrations of the OH radical.[4] It is likely that the actual atmospheric POSF half-life is longer, and potentially much longer, than 3.7 years.

References

[1] T.J. Wallington et al, *J. Chem. Phys. A* 101, pp. 8264-8274 (1997), and references therein.

[2] W.B. DeMore et al, NASA Jet Propulsion Laboratory, JPL Publication No. 94-26 (1994).

[3] M.J. Molina et al , "Atmospheric Lifetime Studies of Some Halogenated Ethers L-14055, L-14056, and L-14093," report to the 3M Specialty Chemicals Division (March 1996).

[4] R.G. Prinn et al, *Science* 269, pp. 187-192 (1995).

[5] The IR absorption cell/reaction chamber is described in United States Patent No. 5,777,735 (1998).

Signatures

Grant M. Plummer, Ph.D., Author — Date: 06/12/01

William K. Reagen, Ph.D., Laboratory Management — Date: 06/12/01

Appendix A: Plots of Infrared Data

Figure A1. Observed Relative Concentrations For Control Conditions C1A and C1B (High UV). UV = 0 for t < 62 min.

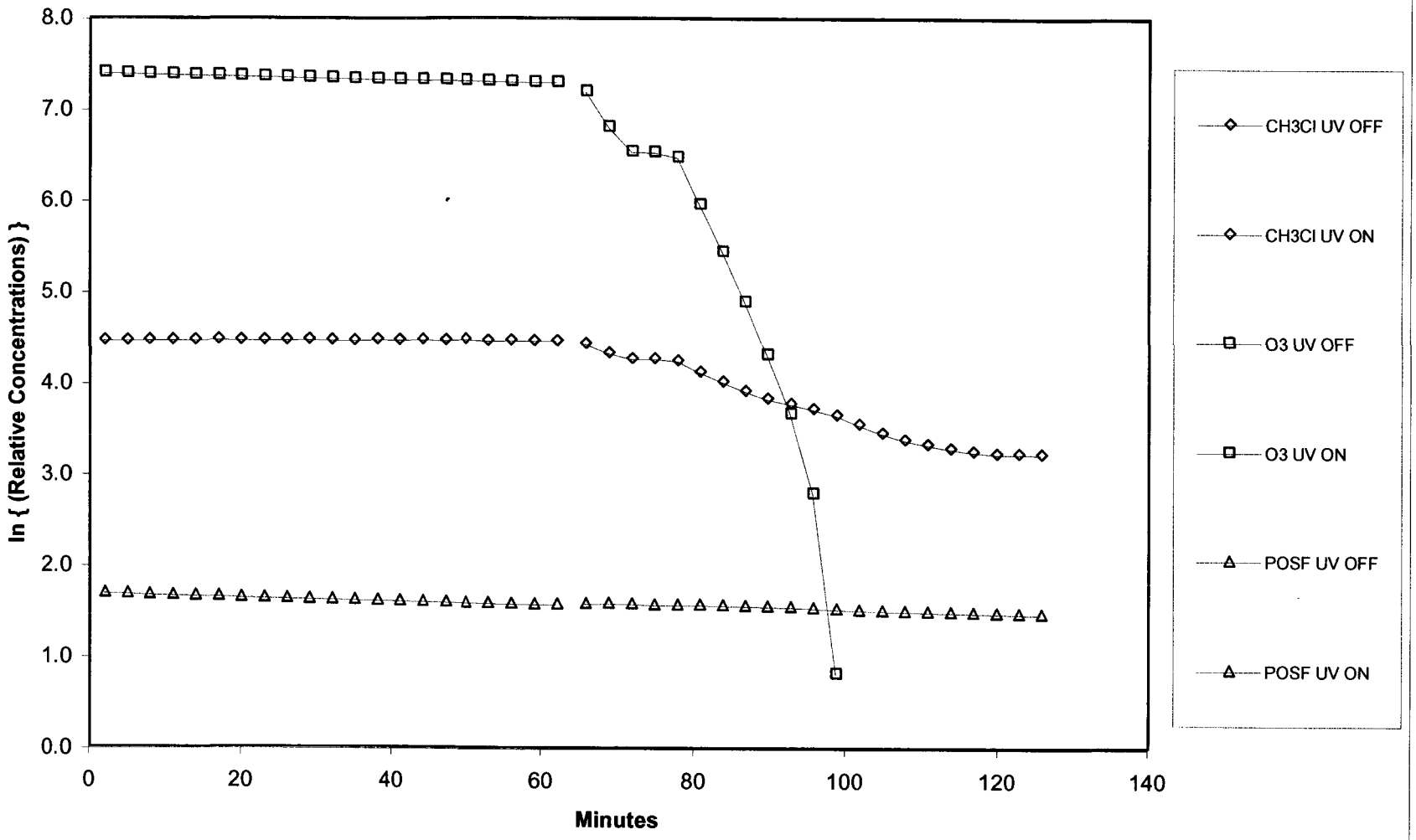

Figure A2. Observed Relative Concentrations For Control Conditions C2A and C2B (High UV). UV = 0 for t < 59 min.

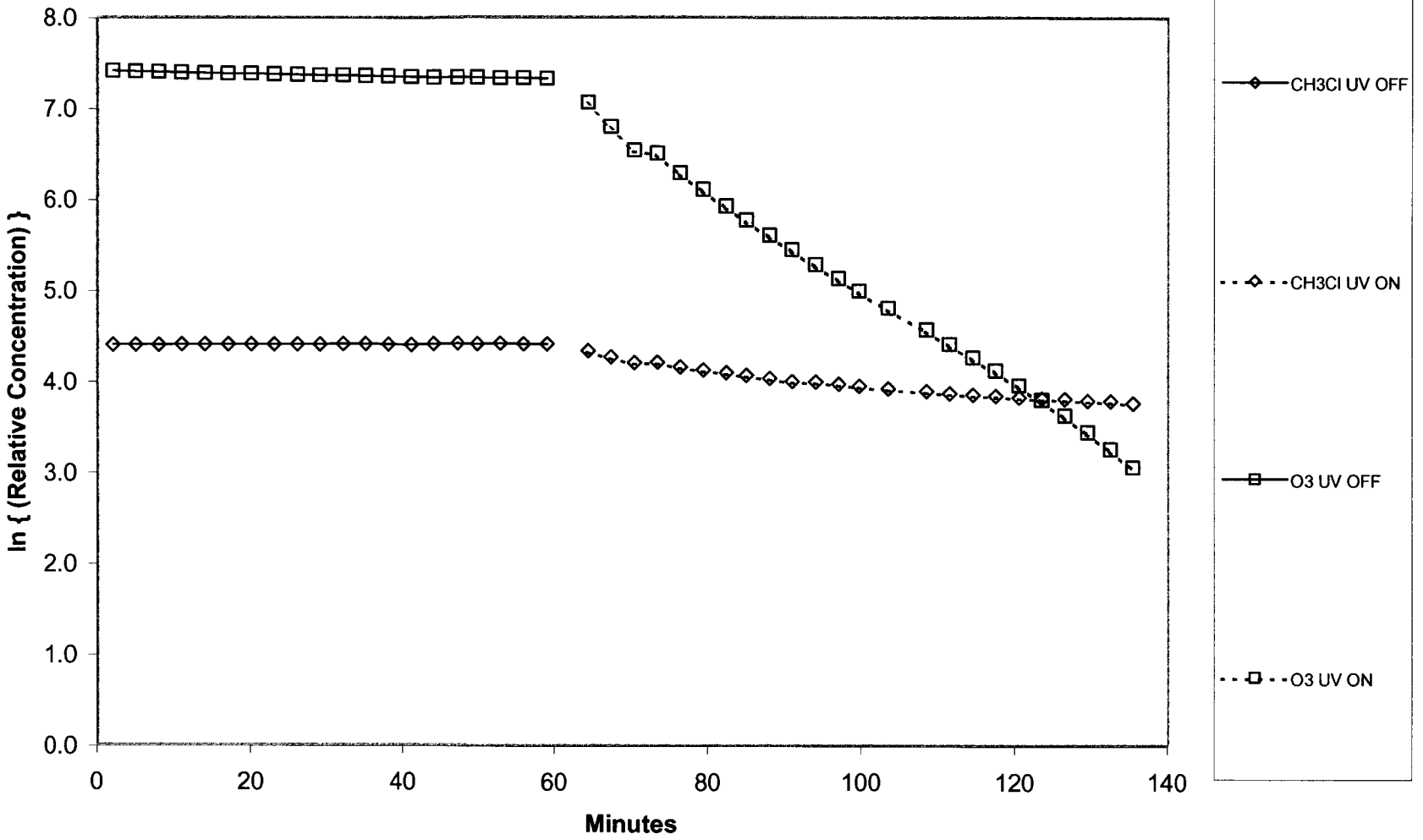

Figure A3. Observed Relative Concentrations For Control Conditions C3A and C3B (Zero Reference Concentration). UV = 0 for t < 127 min.

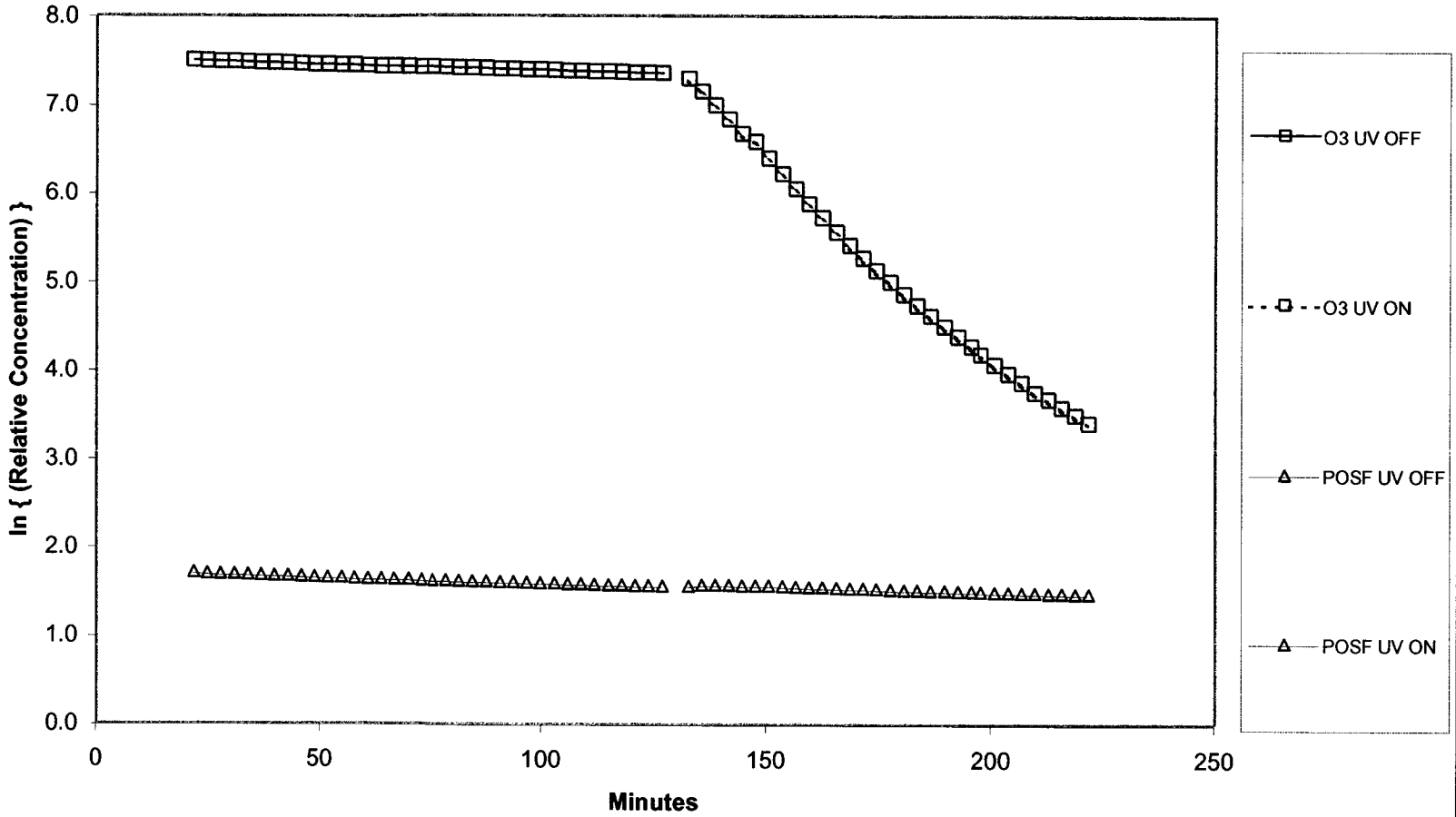

Figure A4. Observed Relative Concentrations For Control Conditions C4A and C4B (High Reference Concentration). UV = 0 for t < 83 min.

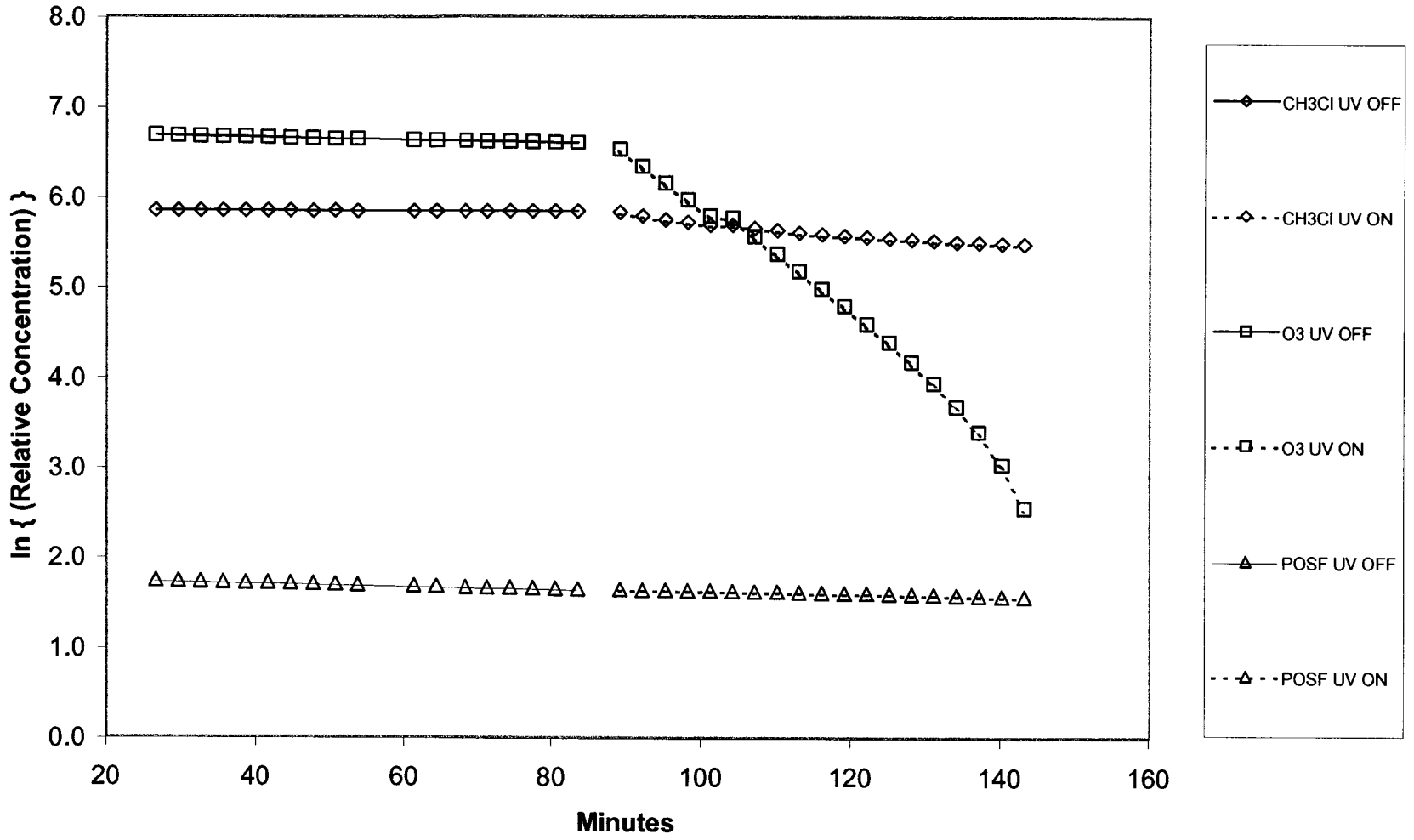

Figure A5. Observed Relative Concentrations For Control Conditions C5A-C5B (High Analyte Concentration). UV = 0 for t < 62 min.

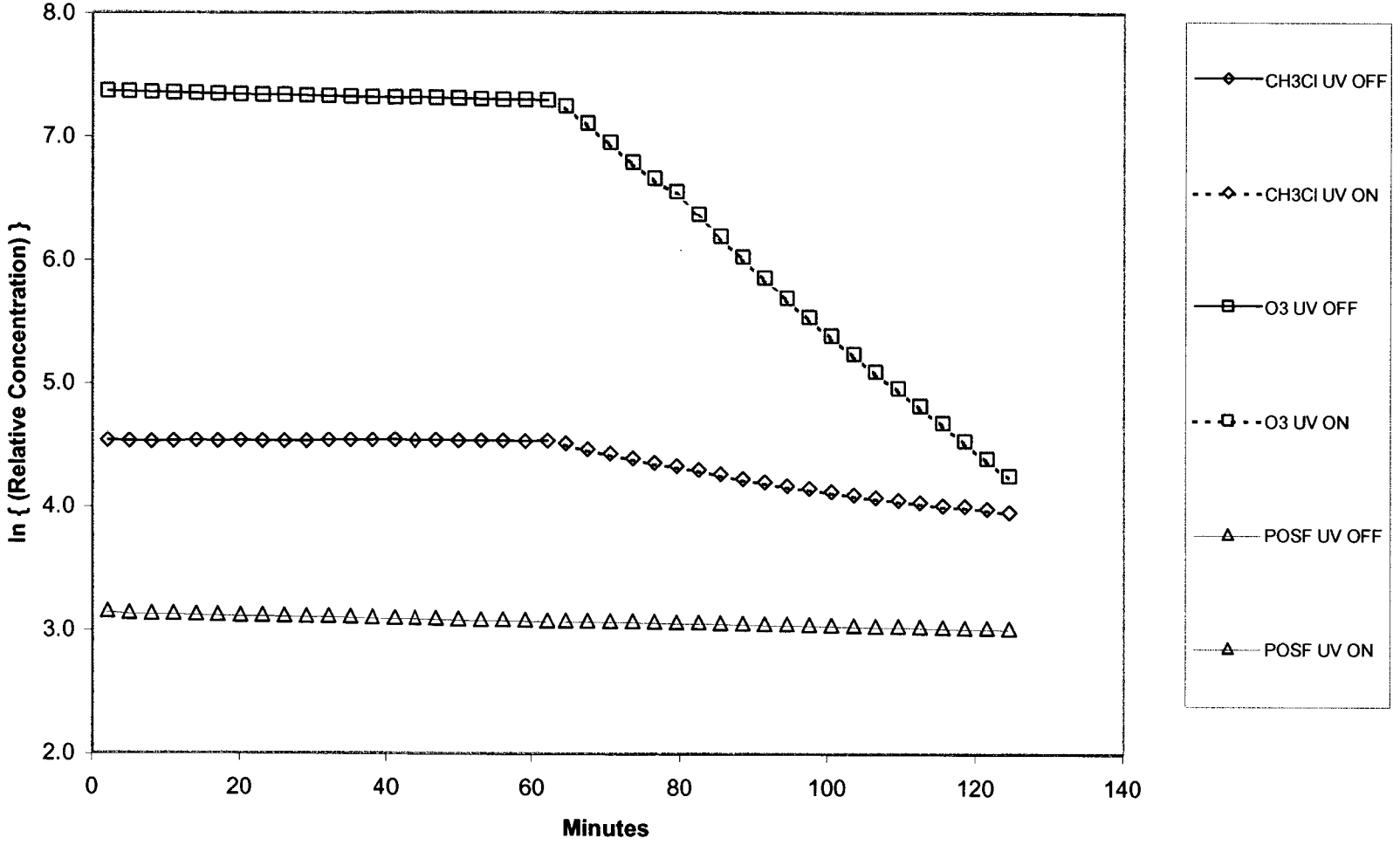

Figure A6. Observed Relative Concentrations For Sample Conditions S1A-S1B. UV = 0 for t < 82 min.

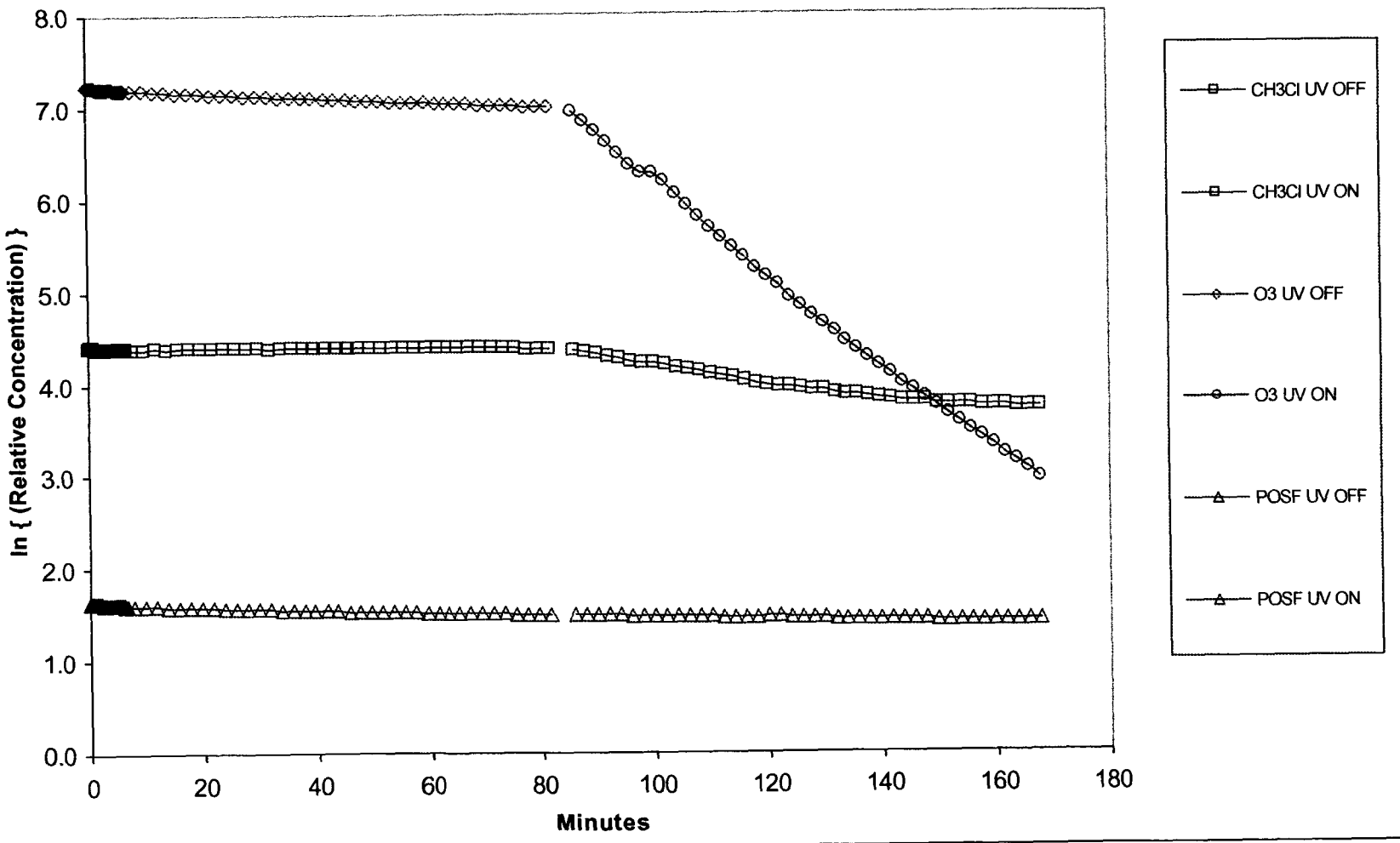

Figure A7. Observed Relative Concentrations For Sample Conditions S2A-S2B. UV = 0 for t < 63 min.

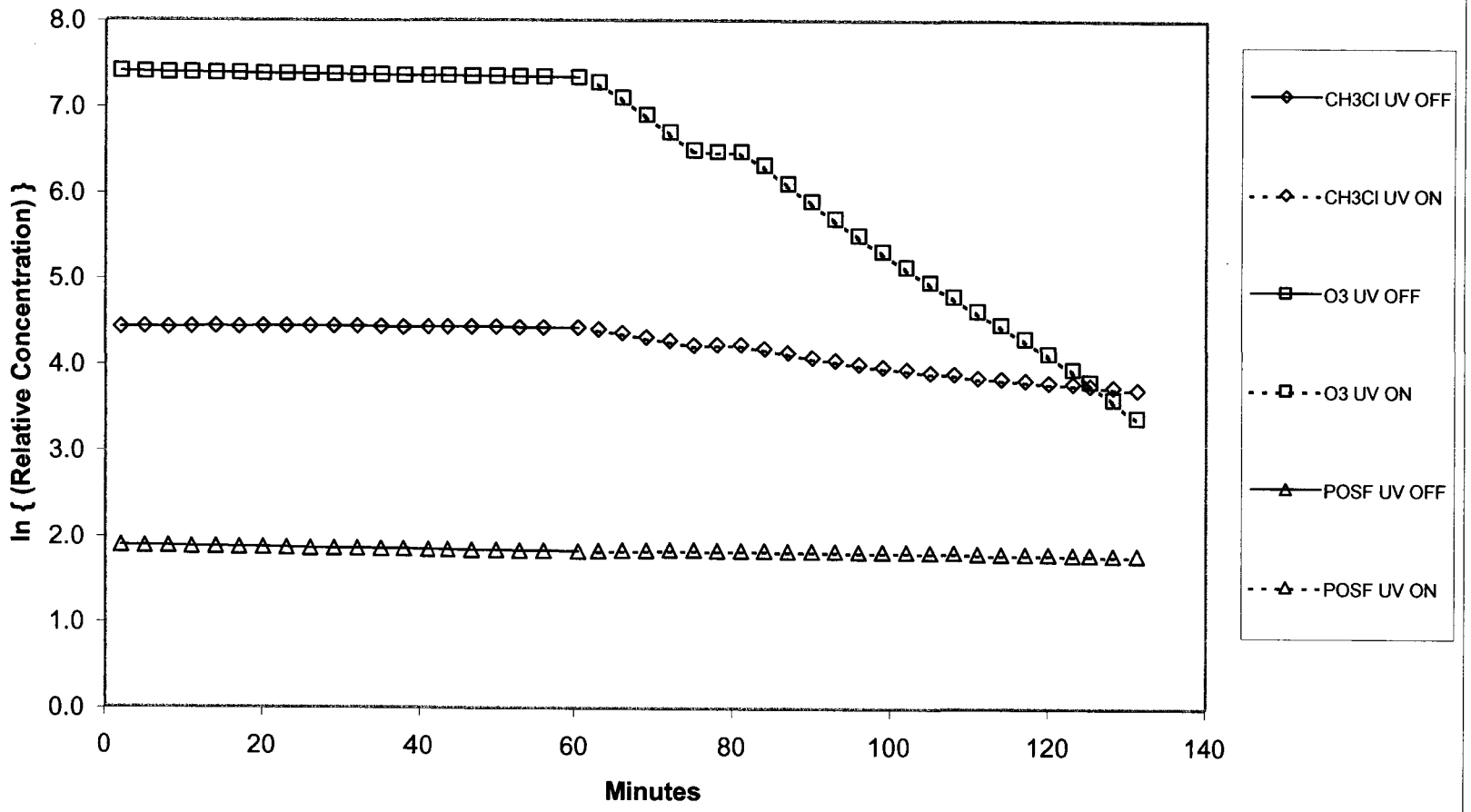

Appendix B: Plots of Least Squares Analyses Data and Results

Figure B1. Observed and Calculated Concentration Ratios For Control Conditions C1A and C1B (High UV). UV = 0 for t < 62 min.

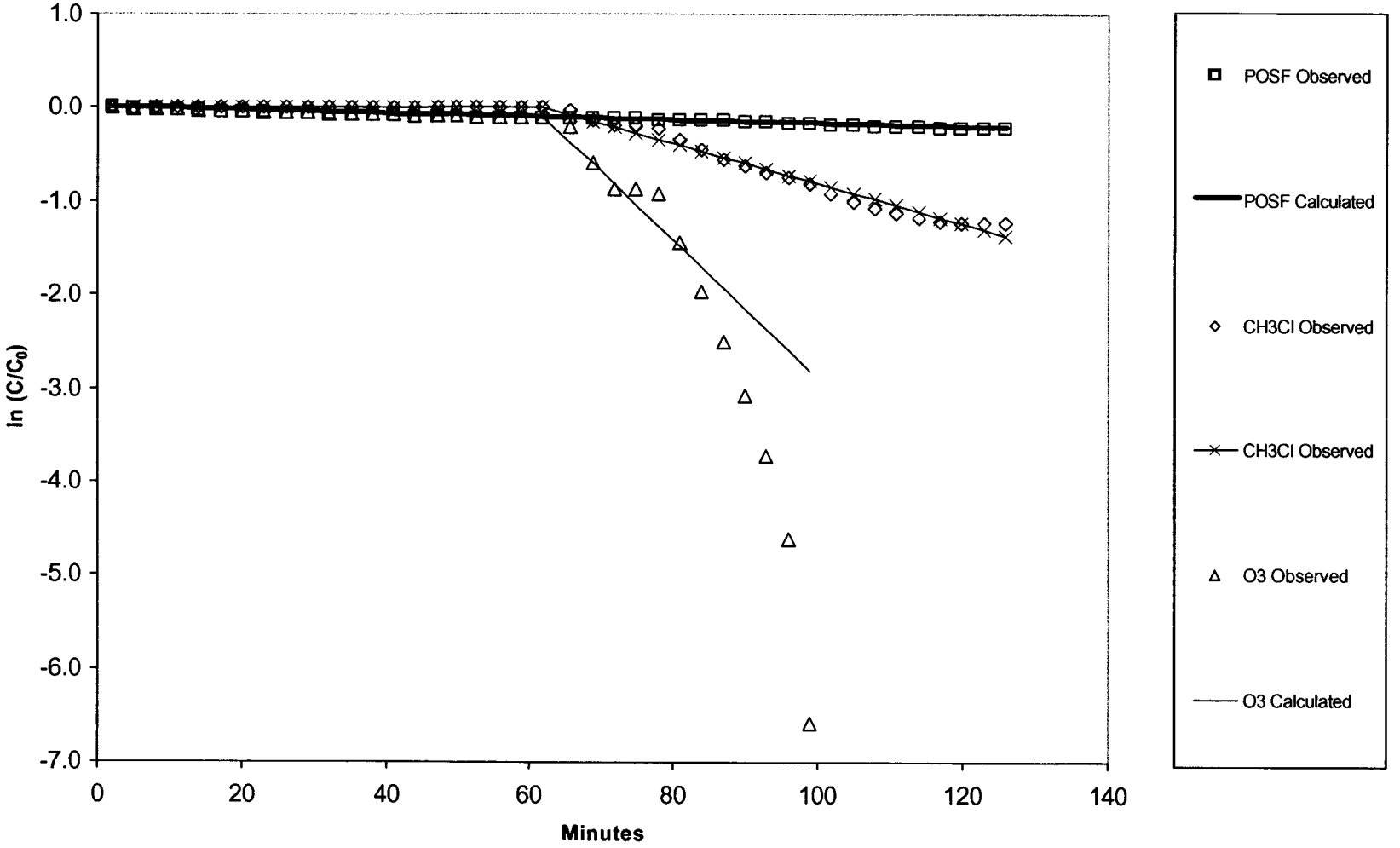

Figure B2. Observed and Calculated Concentration Ratios For Control Conditions C2A and C2B (High UV). UV = 0 for t < 59 min.

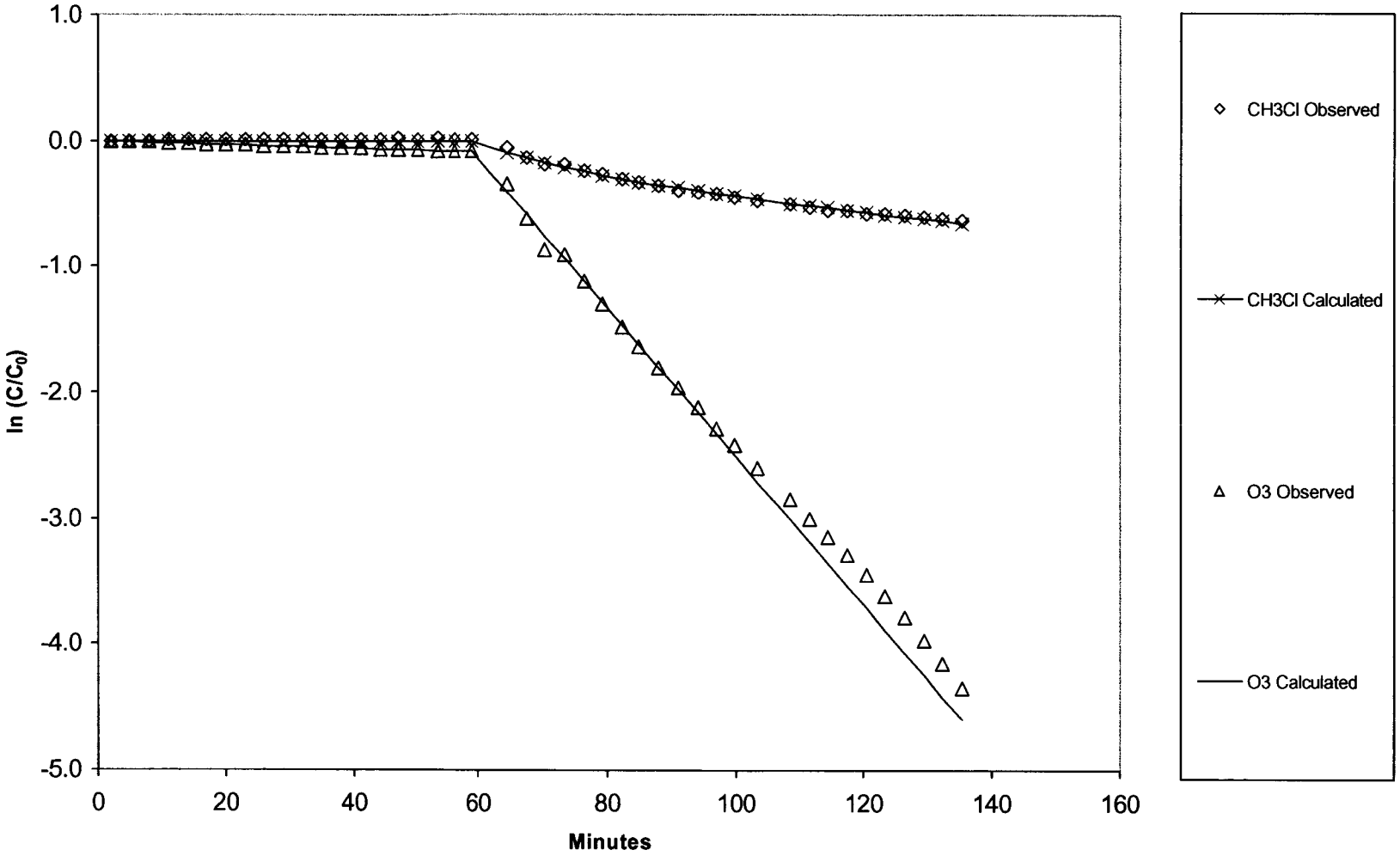

Figure B3. Observed and Calculated Concentration Ratios For Control Conditions C3A and C3B (Zero Reference Concentration). UV = 0 for t < 127 min.

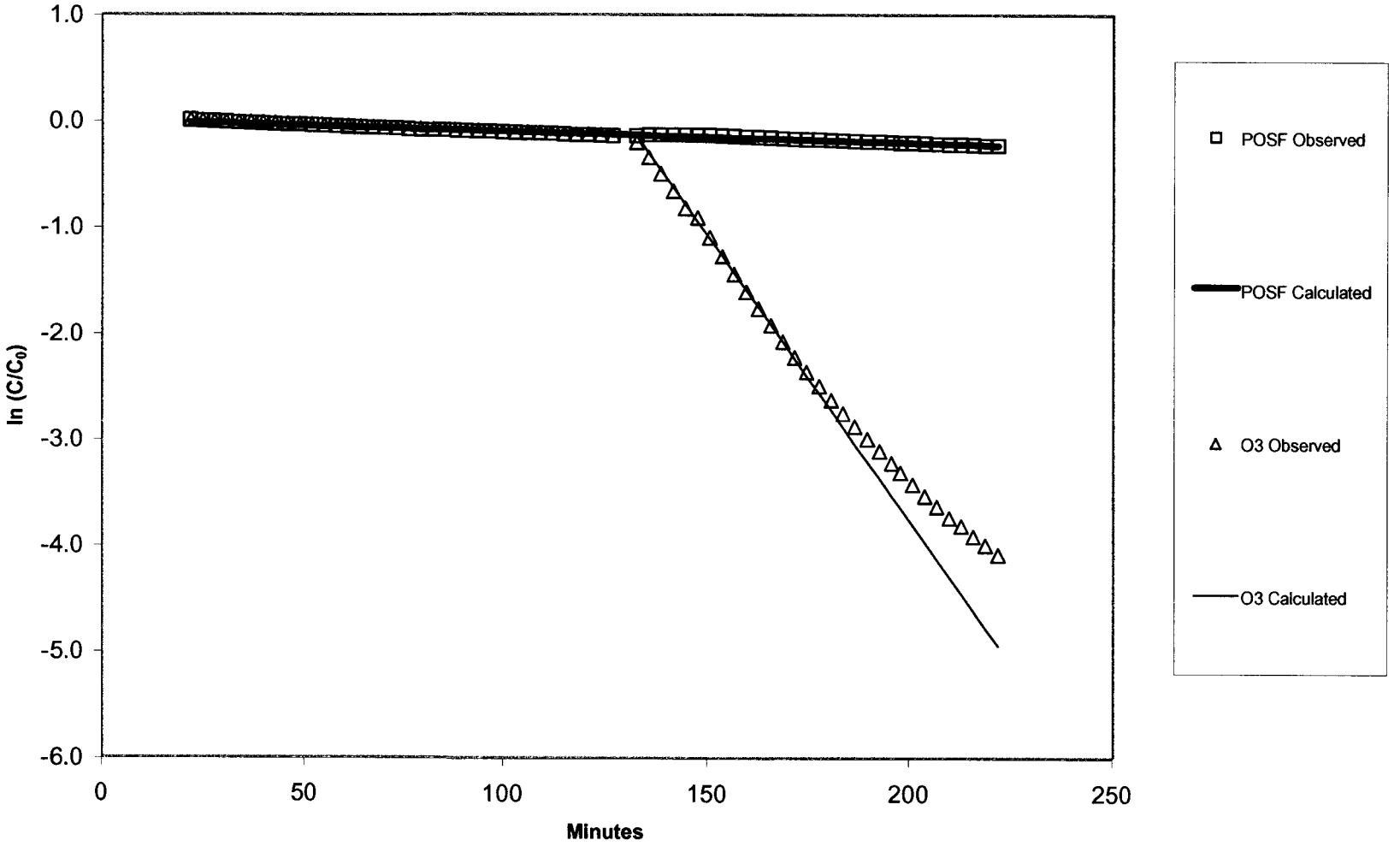

Figure B4. Observed vs. Calculated Concentration Ratios For Control Conditions C4A and C4B (High Reference Concentration). UV = 0 for t < 83 min.

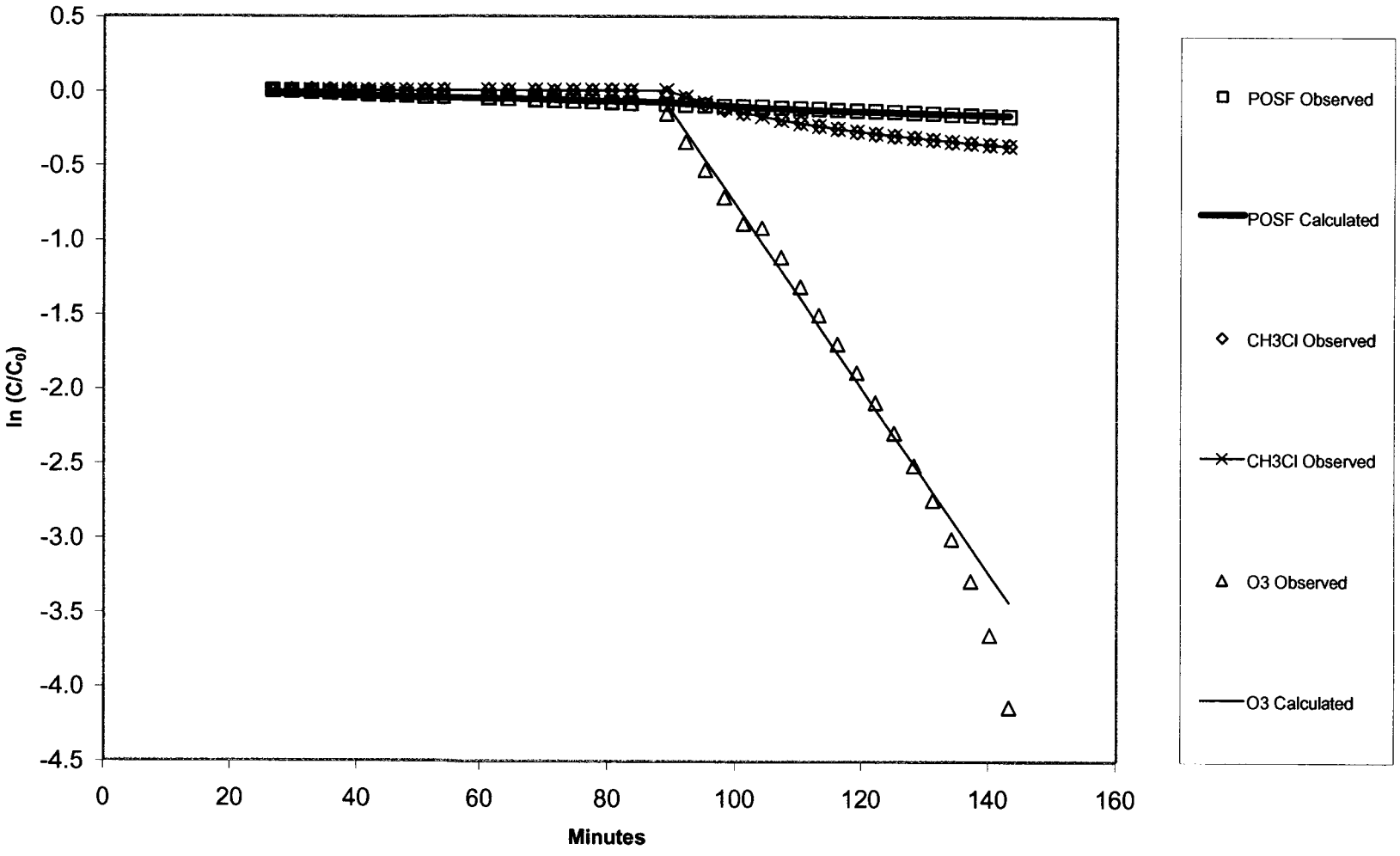

Figure B5. Observed and Calculated Concentration Ratios For Control Conditions C5A-C5B (High Analyte Concentration). UV = 0 for t < 62 min.

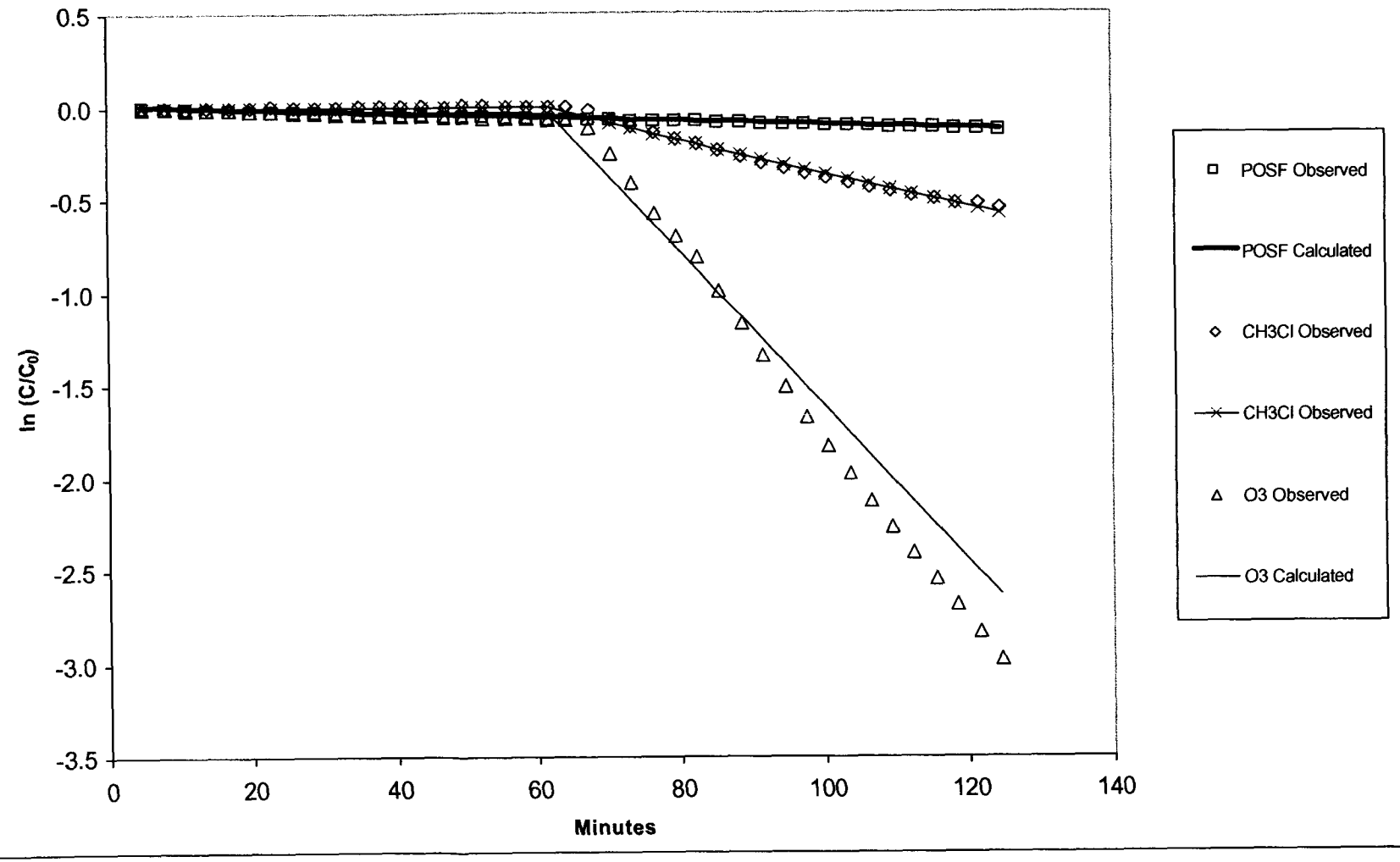

Figure B6. Observed and Calculated Concentration Ratios For Sample Conditions S1A-S1B. UV = 0 for t < 82 min.

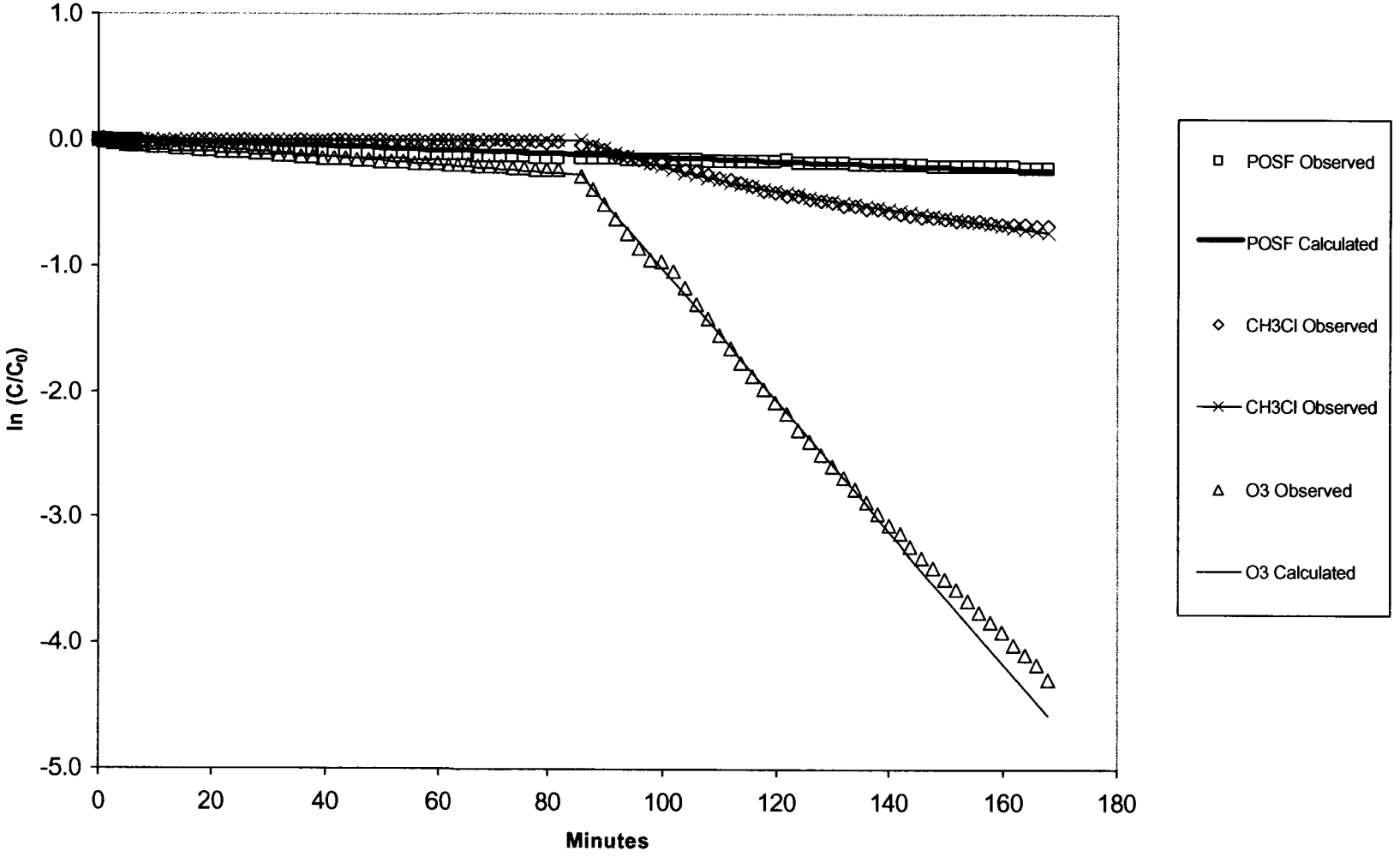

Figure B7. Observed and Calculated Concentration Ratios For Sample Conditions S2A-S2B. UV = 0 for t < 63 min.

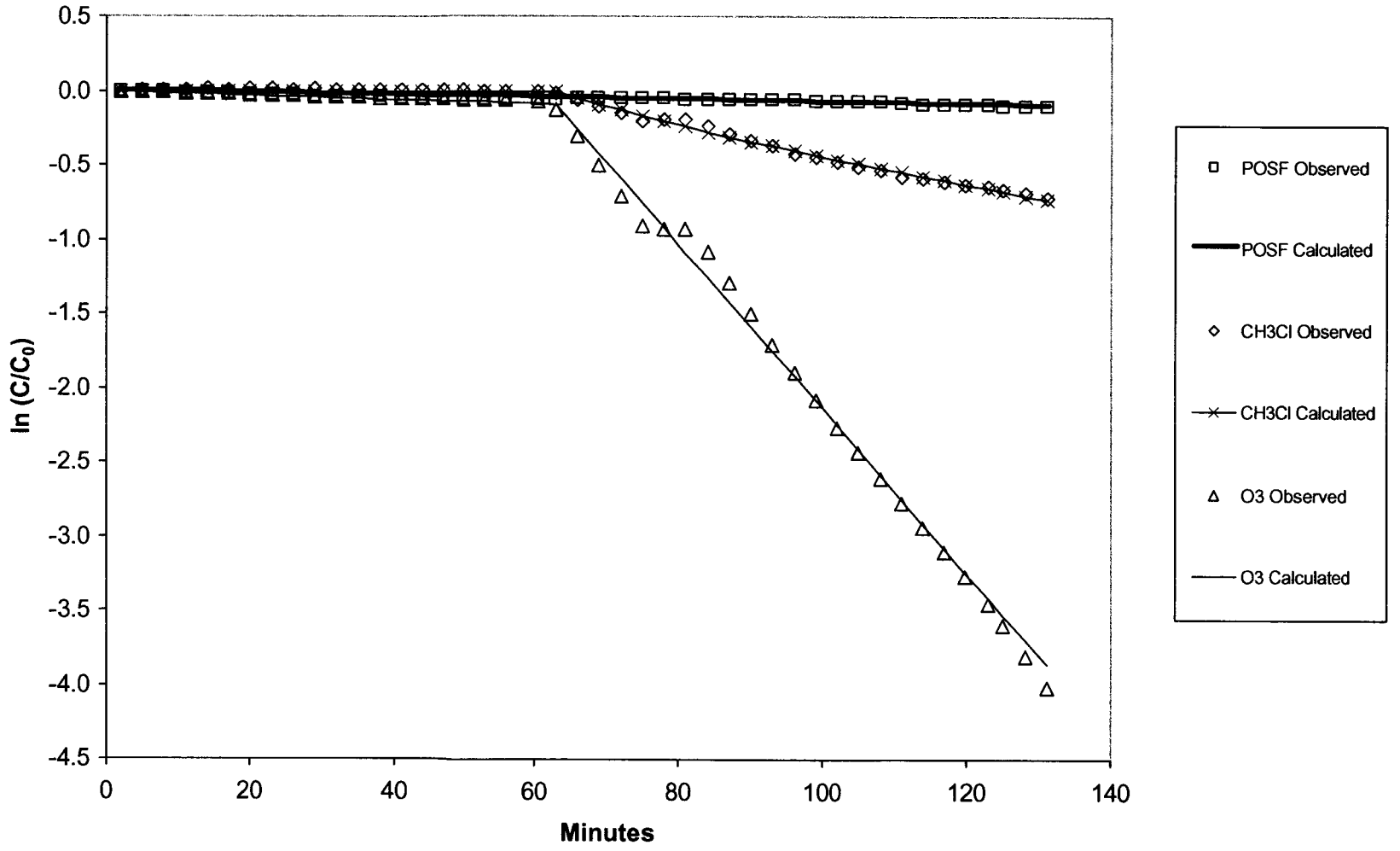

Appendix C: Infrared Reference Spectra and Analytical Regions

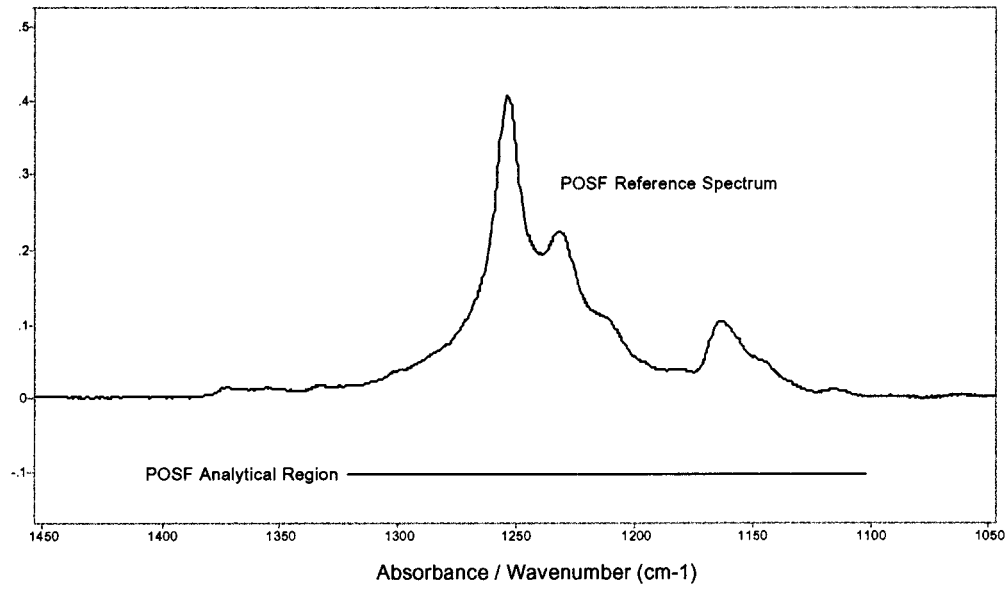
.5
.4
.3
.2
.1
0
-.1
POSF Reference Spectrum
POSF Analytical Region
1450
1400
1350
1300
1250
1200
1150
1100
1050
Absorbance / Wavenumber (cm-1)

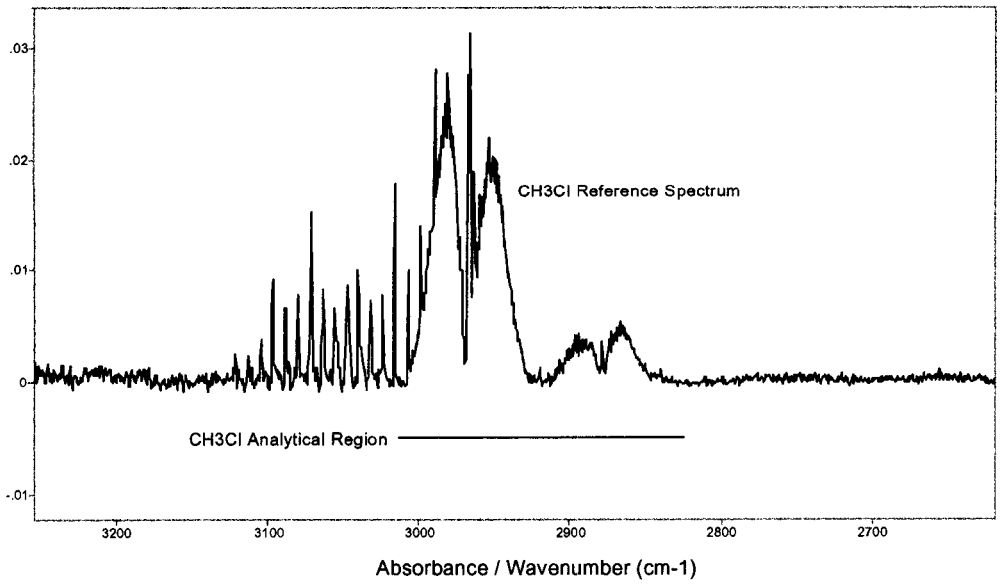
.03
.02
.01
0
-.01
CH3Cl Reference Spectrum
CH3Cl Analytical Region
3200
3100
3000
2900
2800
2700
Absorbance / Wavenumber (cm-1)

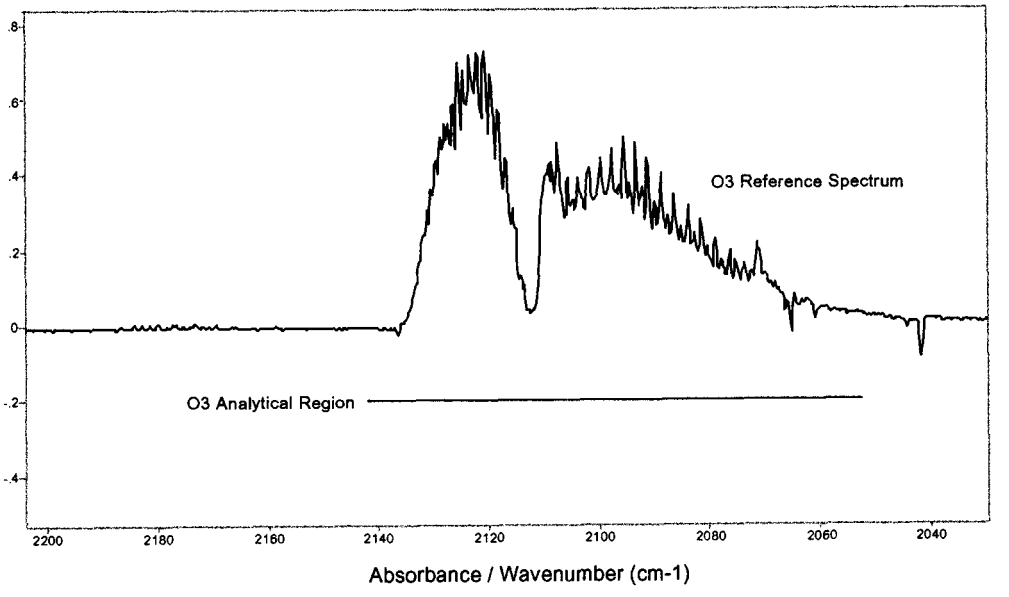
.8
.6
.4
.2
0
-.2
-.4
O3 Reference Spectrum
O3 Analytical Region
2200
2180
2160
2140
2120
2100
2080
2060
2040
Absorbance / Wavenumber (cm-1)